J|A|C|S
ARTICLES
Published on Web 01/22/2004

Comparison of the Kinetics and Thermodynamics for Methyl Radical Addition to C═C, C═O, and C═S Double Bonds

David J. Henry,*,† Michelle L. Coote,*,† Rodolfo Gómez-Balderas,†,‡,§ and Leo Radom*,†,‡

Contribution from the Research School of Chemistry, Australian National University, Canberra, ACT 0200, Australia, and School of Chemistry, University of Sydney, Sydney, NSW 2006, Australia

Received October 20, 2003; E-mail: djhenry@rsc.anu.edu.au; mcoote@rsc.anu.edu.au; radom@chem.usyd.edu.au

Abstract: The barriers, enthalpies, and rate constants for the addition of methyl radical to the double bonds of a selection of alkene, carbonyl, and thiocarbonyl species (CH_2═Z, CH_3CH═Z, and $(CH_3)_2C$═Z, where Z = CH_2, O, or S) and for the reverse β-scission reactions have been investigated using high-level ab inito calculations. The results are rationalized with the aid of the curve-crossing model. The addition reactions proceed via early transition structures in all cases. The barriers for addition of methyl radical to C═C bonds are largely determined by the reaction exothermicities. Addition to the unsubstituted carbon center of C═C double bonds is favored over addition to the substituted carbon center, both kinetically (lower barriers) and thermodynamically (greater exothermicities). The barriers for addition to C═O bonds are influenced by both the reaction exothermicity and the singlet−triplet gap of the substrate. Addition to the carbon center is favored over addition to the oxygen, also both thermodynamically and kinetically. For the thiocarbonyl systems, addition to the carbon center is thermodynamically favored over addition to sulfur. However, in this case, the reaction is contrathermodynamic, addition to the sulfur center having a lower barrier due to spin density considerations. Entropic differences among corresponding addition and β-scission reactions are relatively minor, and the differences in reaction rates are thus dominated by differences in the respective reaction barriers.

Introduction

The addition of carbon-centered radicals to C═C double bonds is an important carbon−carbon bond-forming process and has been investigated widely both by experimental and theoretical procedures.[1] The addition of carbon-centered radicals to C═O bonds has received less attention.[2] However, the reverse reaction, β-scission of alkyl groups from alkoxy radicals (leading to the formation of C═O compounds), has been investigated in more detail due to its importance in atmospheric and combustion chemistry.[3] Recently we have extended our theoretical investigations to the addition of carbon-centered radicals to C═S double bonds,[4] as this is of great importance in the area of reversible addition−fragmentation chain-transfer (RAFT) polymerization.[5]

The barriers and enthalpies for the addition of carbon-centered radicals to double bonds vary markedly for C═C, C═O, and C═S bonds. In general, radical addition to C═S bonds proceeds with low barriers and large exothermicities compared with corresponding additions to C═C and C═O bonds.[1,2,4a] The regioselectivity is also profoundly affected by the nature of the bond, with the sulfur center being the preferred site of attack in addition to C═S bonds, the carbon center being strongly preferred in addition to C═O bonds, and the unsubstituted carbon center being favored in addition to C═C bonds.[1,2c,4a]

† Australian National University.
‡ University of Sydney.
§ On postdoctoral leave from FESC-UNAM (México).

(1) For recent reviews, see for example: (a) Giese, B. *Radicals in Organic Syntheses: Formation of Carbon−Carbon Bonds*; Pergamon: Oxford, 1986. (b) Curran, D. P. In *Comprehensive Organic Sythesis*; Trost, B. M., Flemming, I. M., Semmelhack, M. F., Eds.; Pergamon: Oxford, 1991; Vol. 4. (c) Fossey, J.; Lefort, D.; Sorba, J. *Free Radicals in Organic Chemistry*; Wiley: New York, 1995. (d) Fischer, H.; Radom, L. *Angew. Chem., Int. Ed. Engl.* **2001**, *40*, 1340−1371.

(2) See, for example: (a) Choo, K. Y.; Benson, S. W. *Int. J. Chem. Kinet.* **1981**, *13*, 833−844. (b) Gonzalez, C.; Sosa, C.; Schlegel, H. B. *J. Phys. Chem.* **1989**, *93*, 2435−2440. (c) Che, C.-H.; Zhang, H.; Zhang, X.; Liu, Y.; Liu, B. *J. Phys. Chem. A* **2003**, *107*, 2929−2933. (d) Rauk, A.; Boyd, R. J.; Boyd, S. L.; Henry, D. J.; Radom, L. *Can. J. Chem.* **2003**, *81*, 431−442.

(3) See, for example: (a) Gray, P.; Williams, A. *Chem. Rev.* **1959**, *59*, 239−328. (b) Kochi, J. K. *J. Am. Chem. Soc.* **1962**, *84*, 1193−1197. (c) Lendvay, G.; Viskolcz, B. *J. Phys. Chem. A* **1998**, *102*, 10777−10786. (d) Wilsey, S.; Dowd, P.; Houk, K. N. *J. Org. Chem.* **1999**, *64*, 8801−8811. (e) Caralp, F.; Devolder, P.; Fittschen, C.; Gomez, N.; Hippler, H.; Mereau, R.; Rayez, M. T.; Striebel, F.; Viskolcz, B. *Phys. Chem. Chem. Phys.* **1999**, *1*, 2935−2944. (f) Dibble, T. S. *J. Phys. Chem. A* **1999**, *103*, 8559−8565. (g) Somnitz, H.; Zellner, R. *Phys. Chem. Chem. Phys.* **2000**, *2*, 1899−1905. (h) Somnitz, H.; Zellner, R. *Phys. Chem. Chem. Phys.* **2000**, *2*, 1907−1918. (i) Hippler, H.; Striebel, F.; Viskolcz, B. *Phys. Chem. Chem. Phys.* **2001**, *3*, 2450−2458. (j) Dibble, T. S. *J. Am. Chem. Soc.* **2001**, *123*, 4228−4234. (k) Petraco, N. D. K.; Allen, W. D.; Schaeffer, H. F., III *J. Chem. Phys.* **2002**, *116*, 10229−10237. (l) Ferenac, M. A.; Davis, A. J.; Holloway, A. S.; Dibble, T. S. *J. Phys. Chem. A* **2003**, *107*, 63−72.

(4) (a) Coote, M. L.; Wood, G. P. F.; Radom, L. *J. Phys. Chem. A* **2002**, *106*, 12124−12138. (b) Coote, M. L.; Radom, L. *J. Am. Chem. Soc.* **2003**, *125*, 1490−1491. See also: (c) Macrae, R. M.; Carmichael, I. *J. Phys. Chem. A* **2001**, *105*, 3641−3651.

(5) (a) Chiefari, J.; Chong, Y. K. B.; Ercole, F.; Krstina, J.; Jeffery, J.; Le, T. P. T.; Mayadunne, R. T. A.; Meijs, G. F.; Moad, C. L.; Moad, G.; Rizzardo, E.; Thang, S. H. *Macromolecules* **1998**, *31*, 5559−5562. (b) Destarac, M.; Charmot, D.; Franck, X.; Zard, S. Z. *Macromol. Rapid Commun.* **2000**, *21*, 1035−1039.

 10.1021/ja039139a CCC: $27.50

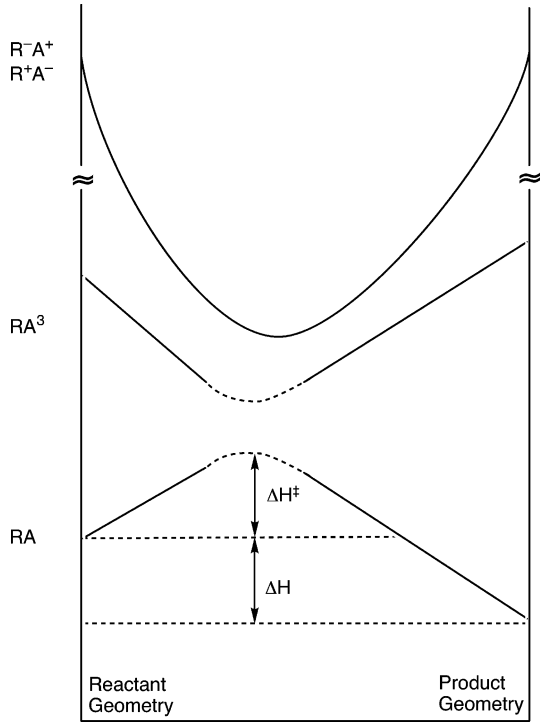

Figure 1. State correlation diagram for the addition of carbon-centered radicals (R) to C═Z double bonds (A).

The barriers, enthalpies, and regioselectivities for addition to the various types of double bonds also show differing sensitivities to substituent effects. Understanding the factors that influence the different behavior of C═C, C═O, and C═S double bonds with respect to radical addition is of interest from a fundamental viewpoint. It also has specific practical importance, for example, in the control of the RAFT polymerization process, as this relies upon a delicate balance of the rates of radical addition to C═C and C═S bonds as well as the reverse (β-scission) reaction in the latter case.

The curve-crossing model (or state correlation diagram)[6] is a powerful theoretical tool, which provides a qualitative framework for the understanding of trends in reaction barriers in terms of the energies of low-lying electronic configurations of reactants and products. This model has previously been applied with great success to the analysis of the barriers for radical additions to alkenes.[1d,6,7] Recently, we also used this model to rationalize the contrathermodynamic behavior in radical additions to alkenes and alkynes.[8] Details of the curve-crossing model have been published elsewhere,[6] but we recap the principal features here in relation to the addition of a radical (R) to an alkene or other unsaturated molecule (A). For these reactions, the four lowest energy doublet configurations are considered (Figure 1). In order of increasing energy at the reactant geometry, these are (a) the configuration of the reactants (RA), (b) the configuration of the products (RA^3), and (c) the two possible configurations arising from charge transfer between the reactants (R^+A^- and R^-A^+). At the transition structure there is a mixing of these configurations, and the barrier ($\Delta H^{\ddagger}$) is determined as a result of an avoided crossing. Three main factors may contribute to lowering the barrier: (a) an increase in the reaction exothermicity (which leads to a lowering of the RA^3 curve at the product end), (b) a decrease in the singlet−triplet gap of the substrate (which leads to a lowering of the RA^3 curve at the reactant end), and (c) the interaction of lower lying charge-transfer configurations.

In the present work, we use the curve-crossing model to rationalize the differences in the barriers, enthalpies, and regioselectivities for methyl radical addition to C═C, C═O, and C═S double bonds. Building upon our earlier separate investigations of the individual systems,[1d,2d,4a,b,7] we compare the barriers and reaction enthalpies for methyl radical addition to each of the centers of selected C═C, C═O, and C═S double bonds using a common high-level ab initio procedure (G3X-RAD//QCISD). We have also calculated the ionization energies (IEs) and electron affinities (EAs) of all the reactants and the singlet−triplet (S−T) gaps of the alkene, carbonyl, and thiocarbonyl species, as these are required in the curve-crossing model in order to analyze the trends observed in the barriers. Additionally, we investigate factors that determine the regioselectivity for the addition of methyl radical to each of the double-bond types. Finally, we have determined frequency factors and reaction rates for each of the addition reactions using simple transition state theory.

Theoretical Procedures

Standard ab initio molecular orbital theory[9] and density functional theory[10] calculations were performed using the GAUSSIAN 98,[11] ACES II 3.0,[12] and MOLPRO 2000.6[13] computer programs. Where methods such as HF, MP2, B3-LYP, and QCISD(T) are written without a prefix, they refer to unrestricted calculations for open-shell systems. In the cases where restricted-open-shell calculations were carried out, they are designated with an 'R' prefix.

Geometries and zero-point vibrational energies (scaled by 0.9776)[14] of reactants, products, and transition structures were determined at the QCISD/6-31G(d) level. In this connection, conformations were screened

(6) See, for example: (a) Pross, A. *Adv. Phys. Org. Chem.* **1985**, *21*, 99−196. (b) Shaik, S. S. *Prog. Phys. Org. Chem.* **1985**, *15*, 197−337. (c) Shaik, S. S.; Canadell, E. *J. Am. Chem. Soc.* **1990**, *112*, 1446−1452. (d) Shaik, S.; Shurki, A. *Angew. Chem., Int. Ed. Engl.* **1999**, *38*, 586−625.
(7) See, for example: (a) Wong, M. W.; Pross, A.; Radom, L. *Isr. J. Chem.* **1993**, *33*, 415−425. (b) Wong, M. W.; Pross, A.; Radom, L. *J. Am. Chem. Soc.* **1994**, *116*, 6284−6292. (c) Wong, M. W.; Pross, A.; Radom, L. *J. Am. Chem. Soc.* **1994**, *116*, 11938−11943.
(8) Gómez-Balderas, R.; Coote, M. L.; Henry, D. J.; Fischer, H.; Radom, L. *J. Phys. Chem. A* **2003**, *107*, 6082−6090.
(9) (a) Hehre, W. J.; Radom, L.; Schleyer; P. v. R.; Pople, J. A. *Ab Initio Molecular Orbital Theory*; Wiley: New York, 1986. (b) Jensen, F. *Introduction to Computational Chemistry*; Wiley: New York, 1999.
(10) See, for example: (a) Parr, R. G.; Yang, W. *Density Functional Theory of Atoms and Molecules*; Oxford University Press: New York, 1989. (b) Koch, W.; Holthausen, M. C. *A Chemist's Guide to Density Functional Theory*; Wiley-VCH: Weinheim, 2000.
(11) Frisch, M. J.; Trucks, G. W.; Schlegel, H. B.; Scuseria, G. E.; Robb, M. A.; Cheeseman, J. R.; Zakrzewski, V. G.; Montgomery, J. A., Jr.; Stratmann, R. E.; Burant, J. C.; Dapprich, S.; Millam, J. M.; Daniels, A. D.; Kudin, K. N.; Strain, M. C.; Farkas, O.; Tomasi, J.; Barone, V.; Cossi, M.; Cammi, R.; Mennucci, B.; Pomelli, C.; Adamo, C.; Clifford, S.; Ochterski, J.; Petersson, G. A.; Ayala, P. Y.; Cui, Q.; Morokuma, K.; Malick, D. K.; Rabuck, A. D.; Raghavachari, K.; Foresman, J. B.; Cioslowski, J.; Ortiz, J. V.; Stefanov, B. B.; Liu, G.; Liashenko, A.; Piskorz, P.; Komaromi, I.; Gomperts, R.; Martin, R. L.; Fox, D. J.; Keith, T.; Al-Laham, M. A.; Peng, C. Y.; Nanayakkara, A.; Challacombe, M.; Gill, P. M. W.; Johnson, B.; Chen, W.; Wong, M. W.; Andres, J. L.; Gonzalez, C.; Head-Gordon, M.; Replogle, E. S.; Pople, J. A. *Gaussian 98*; Gaussian, Inc.: Pittsburgh, PA, 1998.
(12) Stanton, J. F.; Gauss, J.; Watts, J. D.; Nooijen, M.; Oliphant, N.; Perera, S. A.; Szalay, P. G.; Lauderdale, W. J.; Kucharski, S. A.; Gwaltney, S. R.; Beck, S.; Balková, A.; Bernholdt, D. E.; Baeck, K. K.; Rozyczko, P.; Sekino, H.; Hober, C.; Bartlett, R. J. *ACES II*; Quantum Theory Project, University of Florida: Gainsville, FL, 1992.
(13) Werner, H.-J.; Knowles, P. J.; Amos, R. D.; Bernhardsson, A.; Berning, A.; Celani, P.; Cooper, D. L.; Deegan, M. J. O.; Dobbyn, A. J.; Eckert, F.; Hampel, C.; Hetzer, G.; Korona, T.; Lindh, R.; Lloyd, A. W.; McNicholas, S. J.; Manby, F. R.; Meyer, W.; Mura, M. E.; Nicklass, A.; Palmieri, P.; Pitzer, R.; Rauhut, G.; Schütz, M.; Stoll, H.; Stone, A. J.; Tarroni, R.; Thorsteinsson, T. *MOLPRO 2000.6*; University of Birmingham: Birmingham, 1999.
(14) Scott, A. P.; Radom, L. *J. Phys. Chem.* **1996**, *100*, 16502−16513.

at the HF/6-31G(d) level. Barriers and reaction enthalpies were determined at a modified G3X-RAD level,[15] the standard B3-LYP/6-31G(d) geometries and zero-point vibrational energies being replaced by QCISD/6-31G(d) quantities.

Frequency factors and reaction rates for the various addition reactions were obtained via simple transition state theory using scaled (by 1.0187)[14] QCISD/6-31G(d) frequencies. In calculating the entropies of activation, the low-frequency torsional modes were treated as hindered rotors. The rotational potentials associated with these modes were obtained at the QCISD/6-31G(d) level of theory, and the corresponding partition functions and associated thermodynamic properties were then determined via standard methods as follows. For those modes having rotational potentials that could be described by a simple cosine function, the tables of Pitzer and co-workers[16] were used. For the more complex modes, the rotational potentials were fitted with a Fourier series of up to 18 terms, and the corresponding energy levels were then found by numerically solving the one-dimensional Schrödinger equation for a rigid rotor using a Fortran program described previously.[17,18] It should be noted that this more general method yields results identical to those from the Pitzer tables for the particular case of simple cosine rotational potentials. The hindered rotor model, in conjunction with the scaled (by 1.0080) QCISD/6-31G(d) frequencies, was also employed in the calculation of temperature corrections to the barriers and reaction enthalpies.

Vertical triplet excitation energies for the double-bonded substrates were determined at the G3X(MP2)-RAD level.[15] To calculate charge-transfer energies, vertical ionization energies (IEs) and electron affinities (EAs) of all reactants were obtained at a modified G3X(MP2)-RAD level, in which the URCCSD(T)/6-31G(d) and RMP2/6-31G(d) single-point calculations were replaced with URCCSD(T)/6-31++G(d) and RMP2/6-31++G(d), respectively. This modification was found to lead to significantly improved accuracy for several of the anions, and we refer to this modified procedure as G3X(MP2)-RAD(++). As no optimized higher-level correction parameters are available for G3X-(MP2)-RAD(++), we used the G3X(MP2)-RAD values instead. While this may introduce a small error in the individual IE and EA values, this term cancels entirely from the charge-transfer energies used in the curve-crossing model analysis. The extent of charge transfer in the transition structures was established by calculating Bader charges via atoms-in-molecules (AIM) calculations.[19] These were calculated at the UQCISD/6-311+G(d,p)//QCISD/6-31G(d) level, using the correlated (rather than SCF) wave function (i.e., the "density = current" keyword in GAUSSIAN 98). AIM calculations at this level of theory were also used to obtain the spin densities in the triplet states of the various double-bonded substrates.

Results and Discussion

A. Transition Structure Geometries. Schematic transition structure geometries (**1b**−**9b** and **1b′**−**9b′**) and the corresponding product geometries (**1c**−**9c** and **1c′**−**9c′**) for methyl radical addition to the C- and Z-centers of the selected alkene, carbonyl, and thiocarbonyl species (CH_2=Z, CH_3CH=Z, and $(CH_3)_2$-C=Z, where Z = CH_2, O, or S) are shown in Figures 2 and 3, respectively. The principal geometric features of these structures are presented in Table 1.

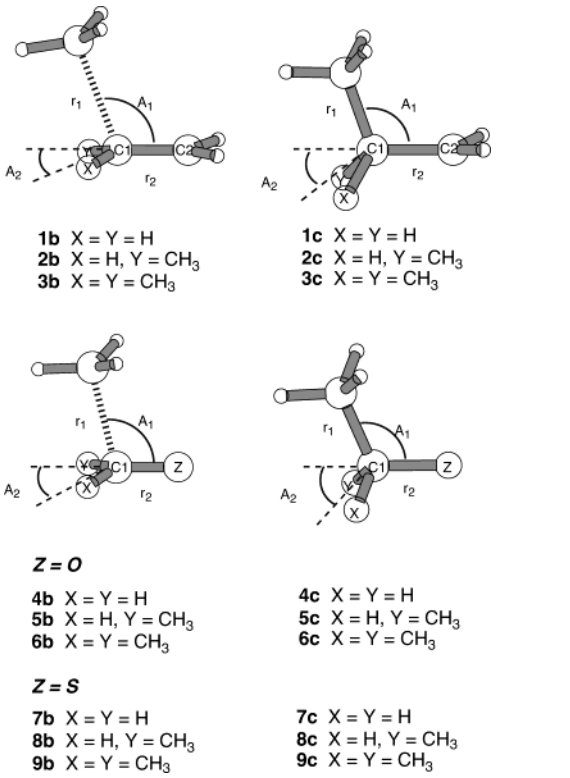

Figure 2. Schematic representation of transition structures and products for methyl radical addition to the carbon center of selected alkene, carbonyl, and thiocarbonyl species.

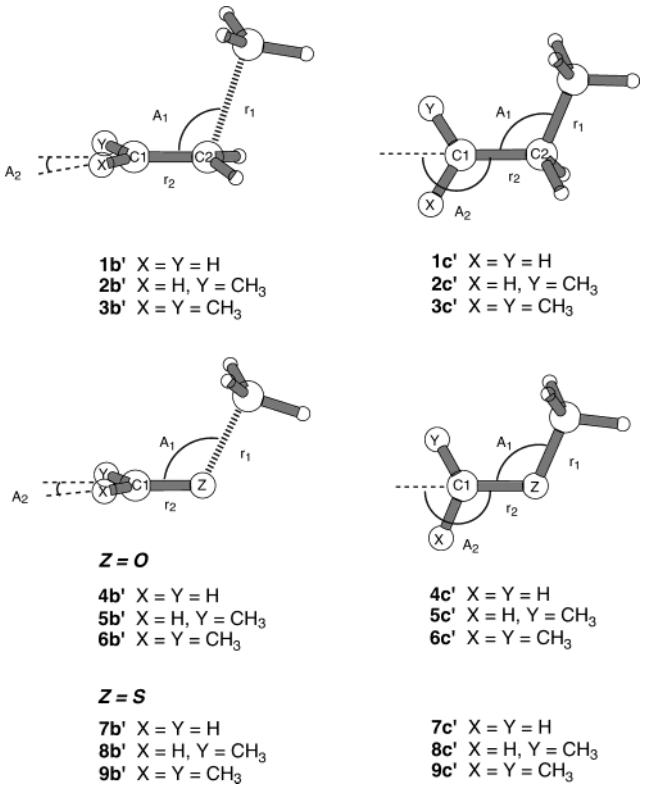

Figure 3. Schematic representation of transition structures and products for methyl radical addition to the Z-center of selected alkene, carbonyl, and thiocarbonyl species.

The addition of methyl radical to either center of the C=C double bond involves an early transition structure, as shown by the long forming C···C bond lengths (r_1). In each of the

(15) (a) Henry, D. J.; Parkinson, C. J.; Radom, L. *J. Phys. Chem. A* **2002**, *106*, 7927−7936. (b) Henry, D. J. Sullivan, M. B.; Radom, L. *J. Chem. Phys.* **2003**, *118*, 4849−4860.
(16) (a) Pitzer, K. S.; Gwinn, W. D. *J. Chem. Phys.* **1942**, *10*, 428−440. (b) Li, J. C.; Pitzer, K. S. *J. Chem. Phys.* **1956**, *60*, 466−474.
(17) (a) Nordholm, S.; Bacskay, G. B. *Chem. Phys. Lett.* **1976**, *42*, 253−258. (b) Bacskay, G. B. Unpublished work.
(18) Heuts, J. P. A.; Gilbert, R. G.; Radom, L. *J. Phys. Chem.* **1996**, *100*, 18997−19006.
(19) See, for example: (a) Bader, R. F. W. *Atoms in Molecules: A Quantum Theory*; Clarendon Press: Oxford, 1990. (b) Stefanov, B. B.; Cioslowski, J. R. *J. Comput. Chem.* **1995**, *16*, 1394−1404 and references therein.

Table 1. Principal Geometric Parameters for the Reactants, Transition Structures, and Product Radicals for the Addition of Methyl Radical to the C- and Z-Centers of C═Z Double Bonds (Z = CH_2, O, and S)[a]

species		r_1	r_2	A_1	A_2
CH_2═CH_2	**1a**		1.338		
CH_3···CH_2═CH_2	**1b**	2.272	1.367	109.5	18.9
$CH_3CH_2CH_2$	**1c**	1.532	1.497	112.9	56.0
CH_3CH═CH_2	**2a**		1.339		
CH_3···CH_3CH═CH_2	**2b**	2.266	1.370	105.2	25.4
$(CH_3)_2CHCH_2$	**2c**	1.534	1.500	111.2	47.0
CH_3CH═CH_2···CH_3	**2b′**	2.276	1.367	109.2	19.2
$CH_3CHCH_2CH_3$	**2c′**	1.531	1.498	113.3	56.5
$(CH_3)_2C$═CH_2	**3a**		1.337		
CH_3···$(CH_3)_2C$═CH_2	**3b**	2.270	1.374	101.2	23.8
$(CH_3)_3CCH_2$	**3c**	1.544	1.504	109.4	35.8
$(CH_3)_2C$═CH_2···CH_3	**3b′**	2.283	1.368	108.8	19.2
$(CH_3)_2CCH_2CH_3$	**3c′**	1.543	1.506	113.3	57.8
CH_2═O	**4a**		1.217		
CH_3···CH_2═O	**4b**	2.125	1.247	102.7	16.4
CH_3CH_2O	**4c**	1.524	1.391	113.8	28.6
CH_2═O···CH_3	**4b′**	1.920	1.271	117.0	5.0
CH_2OCH_3	**4c′**	1.425	1.368	113.6	35.9
CH_3CH═O	**5a**		1.219		
CH_3···CH_3CH═O	**5b**	2.097	1.253	99.7	20.5
$(CH_3)_2CHO$	**5c**	1.530	1.395	111.4	40.5
CH_3CH═O···CH_3	**5b′**	1.901	1.276	116.6	8.3
CH_3CHOCH_3	**5c′**	1.424	1.376	113.6	33.6
$(CH_3)_2C$═O	**6a**		1.223		
CH_3···$(CH_3)_2C$═O	**6b**	2.085	1.260	96.9	24.6
$(CH_3)_3CO$	**6c**	1.536[b]	1.402	107.7[b]	57.2[b]
$(CH_3)_2C$═O···CH_3	**6b′**	1.888	1.281	116.2	11.8
$(CH_3)_2COCH_3$	**6c′**	1.424	1.386	116.3	35.2
CH_2═S	**7a**		1.623		
CH_3···CH_2═S	**7b**	2.461	1.643	107.7	10.0
CH_3CH_2S	**7c**	1.526	1.815	114.7	61.5
CH_2═S···CH_3	**7b′**	2.632	1.635	109.4	1.2
CH_2SCH_3	**7c′**	1.815	1.730	100.3	19.0
CH_3CH═S	**8a**		1.628		
CH_3···CH_3CH═S	**8b**	2.417	1.652	102.4	14.0
$(CH_3)_2CHS$	**8c**	1.532[c]	1.825	109.6[c]	56.5[c]
CH_3CH═S···CH_3	**8b′**	2.596	1.641	108.9	1.8
CH_3CHSCH_3	**8c′**	1.815	1.742	100.1	21.8
$(CH_3)_2C$═S	**9a**		1.636		
CH_3···$(CH_3)_2C$═S	**9b**	2.400	1.663	98.0	17.7
$(CH_3)_3CS$	**9c**	1.535[d]	1.836	108.6[d]	56.0[d]
$(CH_3)_2C$═S···CH_3	**9b′**	2.579	1.649	108.6	2.5
$(CH_3)_2CSCH_3$	**9c′**	1.816	1.757	102.8	25.7

[a] Calculated at the QCISD/6-31G(d) level. Bond lengths in Å, angles in degrees. [b] Average value for Jahn−Teller-distorted structure. Individual values are r_1 = 1.543, 1.532, and 1.532 Å, A_1 = 103.4°, 109.9°, and 109.9°, and A_2 = 52.5°, 59.6°, and 59.6°. [c] Average value for distorted structure. Individual values are r_1 = 1.535 and 1.529 Å, A_1 = 111.4° and 107.8°, and A_2 = 58.6° and 54.4°. [d] Average value for Jahn−Teller-distorted structure. Individual values are r_1 = 1.538, 1.533, and 1.533 Å, A_1 = 105.9°, 109.9°, and 109.9°, and A_2 = 53.2°, 57.4°, and 57.4°.

transition structures considered, the value of r_1 is approximately 1.5 times the length of r_1 in the corresponding product radicals. Other geometric features that indicate an early transition structure include an only marginal increase in the C═C bond lengths (r_2) and the relatively small degree of pyramidalization at the site of attack (A_2) in the transition structures, compared with the corresponding parameters in the product radicals. We note that for addition to the unsubstituted end (C2) of the C═C double bonds (**1b**, **2b′**, **3b′**), the angle of attack (A_1) does not vary significantly with methyl substitution at C1. However, for addition to the substituted end of the selected alkenes (**1b**, **2b**, **3b**), there is a decrease in the angle of attack with increasing methyl substitution, which may reflect increased steric hindrance. Interestingly, for addition to either center of the C═C bonds, the angle of attack in the transition structures is less than the corresponding angle in the product radical.

As shown by the data in Table 1, methyl radical addition to either center of the selected C═O bonds also proceeds via early transition structures (i.e., there is a long forming C···C or C···O bond length (r_1) and only a marginal increase in the C═O bond length (r_2)). For addition to the carbon center, the forming C···C bond length in the transition structures (**4b**−**6b**) is approximately 1.4 times that of the C−C bond length in the product, whereas for addition to the oxygen center, the C···O bond in the transition structures (**4b′**−**6b′**) is approximately 1.3 times that of the C−O length in the product. The angle of approach for methyl addition to the oxygen appears to be relatively insensitive to the presence of methyl substituents at carbon ($A_1 \approx 116-117°$), in a manner similar to that observed for methyl addition to the unsubstituted end of C═C double bonds. In comparison, the angle of approach of the methyl radical for addition to the carbon center decreases on going from formaldehyde, to acetaldehyde, to acetone in a manner similar to that observed for addition to the substituted end of the C═C bonds. For addition to carbon in each of the carbonyl reactions, the angle of attack A_1 and the pyramidalization angle A_2 in the transition structure are both significantly smaller than in the product radical.

Methyl radical addition to C═S double bonds also proceeds via early transition structures, with forming C···C bond lengths to the carbon center of approximately 1.6 times the final bond lengths in the product radicals. For addition to the sulfur center, the forming C···S bond lengths are approximately 1.45 times the product C−S bond lengths. Furthermore, for addition to either end of the selected C═S bonds, there is only a marginal increase in the C═S bond length (r_2) in the transition structures. The angle of approach (A_1) of the methyl radical to the sulfur center of the thiocarbonyls appears relatively insensitive to the presence of methyl substituents at the carbon center. However, the angle A_2 in the transition structures is now noticeably smaller than A_2 in the product radicals. For addition to the carbon center, the angle of approach of the methyl radical in the transition structures decreases with methyl substitution. In each case, both A_1 and A_2 are smaller than in the product radical.

We have noted above that for methyl radical addition to C1 of the selected C═C double bonds, the forming C···C bond length in the transition structure is ∼1.5 times longer than in the product radical, while for addition to C1 of the selected C═O and C═S double bonds, the corresponding C···C distances are ∼1.4 and ∼1.6 times those in the product radicals. In simple geometric terms, this suggests that the transition structures for addition to the carbon center of C═S bonds are slightly earlier than for addition to C═C bonds while those for addition to C═O bonds are slightly later. For addition to the Z-center, we have noted that the forming bond lengths for addition to C═C, C═O, and C═S bonds are, respectively, 1.5, 1.3, and 1.45 times that of r_1 in the corresponding product radicals. This suggests that addition to the Z-center of C═O proceeds via slightly later transition structures than for addition to C═C or C═S bonds. These observations are consistent with considerations based on the reaction exothermicities.

B. Reaction Barriers and Enthalpies. Table 2 presents calculated barriers ($\Delta H_0^{\ddagger}$) and enthalpies (ΔH_0) for addition of methyl radical to a selection of alkenes, carbonyls, and

Table 2. Barriers ($\Delta H_0^{\ddagger}$) and Reaction Enthalpies (ΔH_0) for Methyl Radical Addition to C=Z Double Bonds (Z = CH_2, O, and S) (0 K, kJ mol^{-1})[a]

	add to C		add to Z	
system	$\Delta H_0^{\ddagger}$	ΔH_0	$\Delta H_0^{\ddagger}$	ΔH_0
		Z = CH_2		
CH_2=CH_2	38.4	−87.9	38.4	−87.9
CH_3CH=CH_2	42.3	−84.2	36.7	−88.2
$(CH_3)_2C$=CH_2	46.8	−79.5	34.2	−85.7
		Z = O		
CH_2=O	33.2	−39.2	85.4	−25.0
CH_3CH=O	42.9	−17.0	88.2	−10.2
$(CH_3)_2C$=O	51.4	−5.3	89.7	6.4
		Z = S		
CH_2=S	14.7	−156.0	9.0	−114.1
CH_3CH=S	20.6	−139.2	10.6	−97.8
$(CH_3)_2C$=S	26.5	−129.9	11.3	−85.2

[a] Calculated at the G3X-RAD level on QCISD/6-31G(d) optimized structures.

Table 3. Calculated Relative Energies (eV) of the Triplet Substrate (RA^3)[a] and of the Charge-Transfer Configurations in Methyl Radical (•R) Addition to C=Z Double Bonds (Z = CH_2, O, and S) (A),[b] and Bader Charges on $•CH_3$ in the Corresponding Transition Structures[c]

	substrate			charge-transfer energy[c]		add to C	add to Z
	S–T	IE[d]	EA[e]	R^+A^-	R^-A^+	$q(CH_3)$	$q(CH_3)$
				Z = CH_2			
CH_2=CH_2	4.61	10.83	−1.66	11.48	10.94	−0.02	−0.02
CH_3CH=CH_2	4.62	10.13	−0.78	10.60	10.24	−0.02	−0.03
$(CH_3)_2C$=CH_2	4.62	9.65	−0.70	10.52	9.76	−0.04	
				Z = O			
CH_2=O	3.71	10.97	-0.87	10.69	11.08	+0.08	+0.17
CH_3CH=O	4.07	10.35	-0.72	10.54	10.46	+0.08	+0.16
$(CH_3)_2C$=O	4.24	9.85	-0.59	10.41	9.96	+0.07	
				Z = S			
CH_2=S	2.01	9.39	0.26	9.56	9.50	+0.04	+0.04
CH_3CH=S	2.25	9.01	0.06	9.76	9.12	+0.03	+0.03
$(CH_3)_2C$=S	2.35	8.70	0.04	9.78	8.81	+0.03	

[a] Calculated at the G3X(MP2)-RAD level. [b] Calculated at the G3X(MP2)-RAD(++) level, see text. $IE_v(•CH_3)$ = 9.82 eV, $EA_v(•CH_3)$ = −0.11 eV at this level. [c] Calculated at the UQCISD/6-311+G(d,p)//QCISD/6-31G(d) level. [d] Vertical ionization energy. [e] Vertical electron affinity.

thiocarbonyls (CH_2=Z, CH_3CH=Z, and $(CH_3)_2C$=Z, where Z = CH_2, O, or S), at 0 K. Table 3 displays calculated vertical singlet−triplet gaps (S−T), ionization energies (IEs), and electron affinities (EAs) for each of the substrates and the derived relative energies of the charge-transfer configurations for methyl radical addition to each of the C=Z double bonds, as required for analysis with the curve-crossing model. Also included are the Bader charges on CH_3 in each of the transition structures.

Addition to C=C Double Bonds. The factors contributing to the trends in reaction barriers and enthalpies for radical additions to alkenes have been previously presented in the literature.[1d,7] We therefore discuss them only briefly here in relation to our selected alkenes in order to provide a basis for comparison with the trends and contributing factors for additions to C=O and C=S double bonds.

If we focus first on addition of methyl radical to the substituted carbon center (C1) (Figure 2), we see that the exothermicities decrease with increasing methyl substitution, reflecting hyperconjugative stabilization of the alkene reactants. As predicted by the Evans−Polanyi−Semenov relation[20] and the curve-crossing model, the barriers increase (Table 2). We can also see from Table 3 that, for the three alkenes, the singlet−triplet gap remains relatively constant and the charge-transfer configurations are quite high in energy. This suggests that for these alkenes, the major factor contributing to the observed trend in $\Delta H_0^{\ddagger}$ for addition to C1 is the reaction exothermicities.

In contrast, for the additions to the unsubstituted center (C2) (Figure 2), the increasing hyperconjugative stabilization of the alkene substrates is counteracted by the increasing hyperconjugative stabilization of the product radical. As a result, the variation in both the exothermicities and the barriers are very small, in fact being comparable in size to the estimated mean absolute deviation from experiment for this level of theory.[15b] Nonetheless, previous studies of a wider range of substituted systems have indicated that additions to the unsubstituted center of alkenes are also largely governed by variations in reaction exothermicities.[1d,7]

We can see from Table 3 that for addition to either center of the selected C=C bonds (A), the attacking methyl radical (R) carries only a small charge, indicating that there is relatively little charge transfer in the transition structure. In addition, it is worth noting that for each of the systems, the charge on the attacking methyl in the transition structure is negative and that the R^-A^+ charge-transfer configuration is lower in energy than the R^+A^- configuration. These results all demonstrate that the methyl radical is acting as an electrophile rather than a nucleophile for these reactions. In fact, previous studies have shown that methyl radical tends to exhibit nucleophilic character only for addition to alkenes that bear strongly π-electron-withdrawing substituents.[1d,7a]

While the singlet−triplet gap remains virtually constant for the three alkenes and therefore does not contribute to the barrier trends discussed above, we will see later that the triplet configuration does influence regioselectivity of addition across the C=C double bonds. We should also note that for alkenes with substituents that are more strongly electron-donating or electron-withdrawing than a methyl group, the singlet−triplet gap is likely to show a wider variation than that seen in the present work and therefore may have a greater role in influencing the barriers.

Addition to C=O Double Bonds. The first point that we note is that barriers for addition to the carbon center of the C=O double bonds in formaldehyde, acetaldehyde, and acetone are considerably lower than for addition to the oxygen center. In conjunction with this, we observe that the corresponding reaction exothermicities also favor addition to the carbon center. Che et al.[2c] recently carried out a theoretical investigation of the addition of methyl radical to formaldehyde and similarly found a lower barrier for addition to the carbon center than to the oxygen center.

Looking more closely at the trends for addition to the carbon center, we see that the exothermicities decrease significantly with methyl substitution at C1, this time reflecting strong hyperconjugative stabilization of the carbonyl reactants, and accordingly the barriers increase. The decrease in the exothermicities for the C=O systems (33.9 kJ mol^{-1} overall) is much larger than for the alkenes (8.1 kJ mol^{-1} overall). Not surpris-

(20) (a) Evans, M. G. *Discuss. Faraday Soc.* **1947**, *2*, 271−279. (b) Evans, M. G.; Gergely, J.; Seaman, E. C. *J. Polym. Sci.* **1948**, *3*, 866−879. (c) Semenov, N. N. *Some Problems in Chemical Kinetics and Reactivity* (Engl. Transl.); Princeton Press: Princeton, NJ, 1958; pp 29−33.

ingly, there is also a larger increase in the barriers (18.2 kJ mol^{-1} compared with 8.4 kJ mol^{-1}). The barriers for addition to the oxygen center of the selected C═O double bonds are considerably greater than for addition to the carbon center and again reflect the trends in the exothermicities. However, while there is a large overall decrease in the exothermicities with dimethyl substitution (31.4 kJ mol^{-1}), there is only a relatively small increase in the barriers (4.3 kJ mol^{-1}). This might be reflecting an increasingly important barrier-lowering contribution from charge-transfer configurations (see below).

Unlike the alkenes, the singlet−triplet gap increases significantly from formaldehyde to acetaldehyde to acetone, and as predicted by the curve-crossing model, this should also contribute to the observed increase in the barriers. The importance of the singlet−triplet gap in regard to the barrier heights for addition to the carbon center is demonstrated across the three carbonyl systems. For example, the barrier for addition to the carbon center of formaldehyde is lower than that for addition to ethylene, despite the significantly smaller exothermicity. This may be attributed to the singlet−triplet gap for formaldehyde being 0.9 eV lower than for ethylene and therefore likely to have a greater influence on the barrier. In contrast, for acetone, where the S−T gap is closer to that of the alkenes and the exothermicity is significantly smaller, the barrier is actually higher than for the alkene systems. For acetaldehye, the lower S−T gap but smaller exothermicity appear to balance to give a barrier very similar to that for addition to propene.

The C═O double bond is intrinsically more electronegative than a C═C double bond, even in the absence of strongly electron-donating or electron-withdrawing substituents, and this might be expected to increase the degree of R^+A^- charge transfer in the transition structure. This is indeed indicated by the calculated charges (Table 3) and could be an indication that R^+A^- charge-transfer configuration is contributing to lowering the barrier. The fact that methyl radical carries a positive charge in the transition structure for addition to either center indicates that for these reactions the methyl is now exhibiting nucleophilic character. This is more pronounced for addition to the oxygen. We recently highlighted the importance of significant electron donation by alkyl groups (including methyl) in the β-scission reactions of several alkoxy radicals (including radical **4c′** of the present work) as well as in the alkyl−oxygen bond dissociation energies of related closed-shell systems.[21]

The indication that polar effects might be significant in the case of methyl addition to C═O bonds is in sharp contrast to the case of methyl addition to C═C bonds, despite the fact that the relative energies of the (initial) charge-transfer configurations are similar in both cases. To understand this difference in behavior, it is important to remember that the barrier height is governed by these relative energies *at the transition structure geometries*. While these are certainly related to the relative energies at the reactant geometries, the extent of the contribution of the charge-transfer configurations to the transition structure is also dependent on how the energies of the charge-transfer configurations change relative to the energies of the reactant and product configurations as the reactants approach one another (i.e., the "slopes" in Figure 1[6d]). In the case of methyl addition to C═C bonds, the relatively large reaction exothermicity causes the energy of the product configuration to fall quite sharply as the reactants approach one another, and hence the interaction of this configuration with the reactant configuration provides the dominant effect at the transition structure. As a result, we do not expect polar interactions to be significant in these reactions. In contrast, in the case of addition to C═O bonds, the relatively small reaction exothermicity causes the product configuration to remain relatively high in energy, thereby reducing its interaction with the reactant configuration until further along the reaction coordinate. As a consequence, the relative importance of the more important R^+A^- charge-transfer configuration at the transition structure is increased.

Addition to C═S Bonds. We might expect to observe similar trends for addition of methyl radical to C═S bonds as those noted for the additions to C═O bonds. One aspect that is common to both groups of systems is that the exothermicities indicate that addition to the carbon center is thermodynamically favored. However, in contrast to the carbonyl reactions, the barriers for addition to the heteroatom (i.e., the sulfur center) are lower than for addition to the carbon center. We will discuss this regioselectivity difference in the following section.

Another key difference for the sulfur system is that the barriers for addition to either center of the C═S bonds are considerably smaller than in the corresponding C═C and C═O systems. The lower barriers for these reactions may in part be explained by their very large exothermicity, in accordance with both the curve-crossing model and the Evans−Polanyi−Semenov relation.[20] It is also clear that the thiocarbonyl species have considerably smaller singlet−triplet gaps which, under the curve-crossing model, should also lead to a reduction in the reaction barrier. In fact, the smaller singlet−triplet gaps and greater exothermicities are consistent with the C═S double bonds being weaker than the corresponding C═C and C═O bonds.[22]

Examining the effects of methyl substitution, we see that, for addition to the sulfur center, the barriers are relatively insensitive to the introduction of methyl substituents at the carbon center, increasing only slightly (by approximately 2 kJ mol^{-1}) across the series. As noted earlier, the barriers for addition to the oxygen center of the C═O bonds also display only a slight sensitivity to methyl substitution, increasing by ~4 kJ mol^{-1} across the series. The exothermicities for addition to sulfur, while being significantly greater than for the corresponding carbonyl reactions, decrease across the series to a similar extent (29.7 kJ mol^{-1}, compared with 31.4 kJ mol^{-1} for the carbonyl series). The effects of methyl substitution for addition to the carbon center of the thiocarbonyl systems are also similar to the analogous alkene and carbonyl species, with the exothermicities decreasing across the series while the corresponding barriers increase.

The charge-transfer configurations for these reactions are lower in energy than those for the corresponding C═C and C═O reactions. However, the exothermicities are considerably greater in the C═S reactions and, based on the discussion in the

(21) (a) Coote, M. L.; Radom, L. *Macromolecules* **2003**, in press. (b) Coote, M. L.; Pross, A.; Radom, L. *Org. Lett.* **2003**, *5*, 4689−4672. (c) Coote, M. L.; Pross, A.; Radom, L. In *Fundamental World of Quantum Chemistry: A Tribute to the Memory of Per-Olov Löwdin;* Brändas, E. J., Kryachko, E. S., Eds.; Kluwer-Springer: New York, submitted for publication; Vol. 3.

(22) See, for example: (a) Schleyer, P. v. R.; Kost, D. *J. Am. Chem. Soc.* **1988**, *110*, 2105−2109. (b) Hadad, C. M.; Rablen, P. R.; Wiberg, K. B. *J. Org. Chem.* **1998**, *63*, 8668−8681. (c) Schmidt, M. W.; Truong, P. H.; Gordon, M. S. *J. Am. Chem. Soc.* **1987**, *109*, 5217−5227.

previous section, we might therefore expect this to offset (at least to some extent) the lower initial value for the charge-transfer energy in the present case. Examining the charges in the transition structure, we note that the charge separation is indeed small. Interestingly, for addition to either center, the methyl radical carries a very small *positive* charge. This is despite the fact that the R^-A^+ charge-transfer configuration (i.e., where methyl radical acts as an electron acceptor) is lower in energy than the R^+A^- configuration. However, the difference in energies of the initial R^-A^+ and R^+A^- configurations is relatively small (especially for the unsubstituted system), so both configurations may contribute to the transition structure (leading consequently to the observed small overall charge transfer). It is therefore possible that the charge-transfer configurations are contributing to some extent to the barrier lowering, despite the small amount of charge separation. Indeed, it may be that a lowering of the barriers associated with increasing contributions of charge-transfer configurations with increasing methyl substitution is offsetting the increase in barriers expected on the basis of increasing singlet−triplet gap and decreasing exothermicity, leading to the small overall changes. A consideration of the effects of electron-donating and -withdrawing substituents on the charges and barriers would provide useful additional information regarding the importance of polar effects in these reactions.

C. Regioselectivity. In the previous section, we saw that there appears to be a preference for addition of methyl radical to the unsubstituted end of C═C double bonds bearing one or two methyl substituents. Shaik and Canadell[6d] rationalized such regioselectivity in radical additions to substituted alkenes in terms of the spin density distribution in the triplet states of the alkenes. Specifically, they argued that a stronger early bonding interaction occurs for methyl radical addition to the site of greater spin density, which in turn leads to a steeper slope for the RA^3 curve, less distortion before the RA curve reaches resonance with the RA^3 curve, i.e., an earlier TS with a longer forming C···C bond, and hence a lower barrier. Alternatively, lower spin density at C1 leads to a decrease in the initial slope of the triplet curve, a later transition structure, i.e., a shorter forming C···C bond length, and therefore a higher barrier.

Clearly, in the symmetrical case of ethylene, the triplet state involves one electron being located on each carbon and the spin density at each carbon is identical. However, introduction of a substituent at C1 leads to an imbalance of the spin density at C1 and C2 and hence a spin density contribution to regioselectivity. Shaik and Canadell[6d] use simple valence-bond (VB) arguments to demonstrate, for example, that a π-electron-donating substituent X (e.g., X = F, Cl, OR, or methyl) leads to greater spin density on the unsubstituted carbon (C2) than on the substituted carbon (C1). They suggest that if the regioselectivity predictions based on spin densities and reaction enthalpies coincide, then the situation should be reasonably clear-cut. However, if the regioselectivity predictions do not coincide, then the situation is less straightforward.

Table 4 presents spin densities for the vertical triplet states of each of the C═C, C═O, and C═S species considered in this study. The results for the alkenes clearly indicate greater spin density at the unsubstituted carbon C2 (Z) for the two substituted systems ($CH_3CH═CH_2$ and $(CH_3)_2C═CH_2$), so this is predicted to be the preferred site for addition of methyl radical on the basis of spin density considerations. In this case, the calculated exothermicities also favor addition to the unsubstituted carbon, and indeed the lower barriers are found for reaction at this position. Furthermore, the forming C···C bond lengths (r_1) in transition structures **2b′** and **3b′** (for addition to the unsubstituted carbon) are in fact slightly greater than those in the transition structures **2b** and **3b** (for addition to the substituted carbon), reflecting the earlier transition structures.

Table 4. Spin Densities on the C and Z Centers of the Vertical Triplet States of the Various C═Z Substrates[a]

	C	Z
	Z = CH_2	
$CH_2═CH_2$	0.979	0.979
$CH_3CH═CH_2$	0.910	0.977
$(CH_3)_2C═CH_2$	0.853	0.971
	Z = O	
$CH_2═O$	0.715	1.042
$CH_3CH═O$	0.687	1.030
$(CH_3)_2C═O$	0.659	1.023
	Z = S	
$CH_2═S$	0.720	1.180
$CH_3CH═S$	0.709	1.153
$(CH_3)_2C═S$	0.693	1.134

[a] Calculated at the QCISD/6-311+G(d,p)//QCISD/6-31G(d) level.

The situation for addition to the C═O and C═S bonds is somewhat more complicated, as the spin-density and exothermicity effects oppose one another. In each case, the spin densities in the triplet are greater on the heteroatom than on the carbon, thereby favoring addition to the heteroatom. In contrast, the exothermicities favor addition to the carbon center in each case. For the C═O reactions, addition to the C-center is preferred and hence we can conclude that the exothermicity effects are dominant. In addition, the mixing coefficient for the interaction of the charge-transfer configurations with the reactant configuration will depend on the frontier molecular orbitals.[1d] In the case of the nucleophilic addition of the methyl radical to C═O bonds, the lowest unoccupied molecular orbital (LUMO) is relevant and this is concentrated on carbon. Such considerations would thus also favor the observed strong preference for addition to C compared with O. In contrast, for the C═S reactions, addition to the S-center is preferred and hence we can conclude that the spin-density effects dominate these latter reactions. The greater importance of the spin-density effects in the C═S reactions (compared with the C═O reactions) may be partly due to the considerably lower singlet−triplet gap in the former case, as this in turn should lead to the triplet configuration dominating the reaction at an earlier stage.

D. Kinetics. Arrhenius preexponential factors (A), activation energies (E_a), and corresponding rate constants (k) at 298 K for methyl radical addition to the C- and Z-center of the selected alkene, carbonyl, and thiocarbonyl species ($CH_2═Z$, $CH_3CH═Z$, and $(CH_3)_2C═Z$, where Z = CH_2, O, or S) are shown in Table 5. Corresponding values for the reverse (β-scission) reactions are shown in Table 6.

Examining first the addition reactions, we note that the preexponential factors for all of the reactions lie in a relatively small range. There is a small entropic preference (i.e., larger A) for addition to the unsubstituted carbon (in the case of the alkenes) or heteroatom Z (in the case of the carbonyl and thiocarbonyl compounds), and this preference increases with increasing methyl substitution. This is a result of the increased

Table 5. Arrhenius Preexponential Factors (log(A/L mol^{-1} s^{-1})), Activation Energies (E_a, kJ mol^{-1}), and Rate Constants (log(k/L mol^{-1} s^{-1}) for Methyl Radical Addition to C=Z Double Bonds (Z = CH_2, O, and S) at 298 K

	add to C			add to Z		
system	log A	E_a	log k	log A	E_a	log k
		Z = CH_2				
CH_2=CH_2	8.7	37.8	2.1	8.7	37.8	2.1
CH_3CH=CH_2	7.8	42.4	0.4	8.2	37.0	1.7
$(CH_3)_2C$=CH_2	7.7	46.8	−0.5	8.6	35.2	2.4
		Z = O				
CH_2=O	8.1	31.8	2.6	8.3	84.1	−6.5
CH_3CH=O	7.4	42.2	0.0	7.8	88.4	−7.7
$(CH_3)_2C$=O	7.1	51.0	−1.8	8.2	89.9	−7.6
		Z = S				
CH_2=S	8.7	14.5	6.1	9.1	9.6	7.4
CH_3CH=S	8.0	21.2	4.3	8.7	11.6	6.6
$(CH_3)_2C$=S	7.8	27.2	3.0	9.0	12.8	6.8

Table 6. Arrhenius Preexponential Factors (log(A/L mol^{-1} s^{-1})), Activation Energies (E_a, kJ mol^{-1}), and Rate Constants (log(k/L mol^{-1} s^{-1}) for β-Scission of the Product Radicals to Re-Form C=Z Double-Bonded Reactants (CH_2=Z, Z = CH_2, O, and S) at 298 K[a]

	CH_3–C(X,Y)Z• (product of addition to C)			•C(X,Y)Z–CH_3 (product of addition to Z)		
system	log A	E_a	log k	log A	E_a	log k
		Z = CH_2				
CH_2=CH_2	13.1	129.4	−9.6	13.1	129.4	−9.6
CH_3CH=CH_2	13.5	130.0	−9.2	13.1	128.1	−9.3
$(CH_3)_2C$=CH_2	14.0	130.3	−8.8	13.2	122.6	−8.3
		Z = O				
CH_2=O	13.7	75.9	0.4	13.7	113.1	−5.5
CH_3CH=O	13.9	63.9	2.7	13.6	101.1	−4.1
$(CH_3)_2C$=O	13.9	60.8	3.3	14.0	86.0	−1.0
		Z = S				
CH_2=S	14.4	175.3	−16.3	13.9	127.2	−8.3
CH_3CH=S	14.5	164.9	−14.4	13.8	111.5	−5.7
$(CH_3)_2C$=S	14.7	162.1	−13.7	14.0	99.7	−3.5

[a] Low-frequency torsional modes treated as hindered rotors.

steric hindrance for addition at the substituted carbon/heteroatom, which leads to a reduced vibrational entropy of activation. In contrast, for addition to the unsubstituted center, methyl substitution has a favorable effect on the vibrational entropy due to the increased degrees of freedom. However, even in this latter case, methyl substitution reduces the overall preexponential factor for the reactions because the substituted systems have a reduced rotational entropy of activation.

We also note that the preexponential factors for addition to the carbonyl compounds are slightly lower than for addition to the alkenes, while those for addition to the thiocarbonyl compounds are slightly higher (especially for addition to the sulfur). These differences arise mainly in the vibrational entropy of activation and are probably associated with the differing lengths of the forming bonds in their respective transition structures (C···S > C···C > C···O). Apart from inherent differences in C−Z bond lengths, in the case of addition to the carbonyl compounds, the transition structures are relatively late (i.e., shorter forming bonds) and this would lead to increased steric hindrance, compared with the corresponding alkene additions. In contrast, the transition structures for addition to the thiocarbonyl compounds are relatively early and should therefore experience reduced steric hindrance.

Despite small differences in their preexponential factors, the relative rate constants of methyl radical addition to (either side of) the various substrates are generally dominated by differences in the reaction barriers. Hence, additions to thiocarbonyl compounds are relatively fast at room temperature and prefer the sulfur center. Additions to carbonyl compounds and alkenes are significantly slower and prefer the carbon center and the unsubstituted carbon centers, respectively. In the unsubstituted cases, addition to formaldehyde is slightly faster than addition to ethylene. However, with increasing methyl substitution, the rates for addition to the alkenes become significantly higher. It is worth noting that Che et al.[2c] found in a theoretical investigation of the reaction of methyl radical with formaldehyde that the rate for hydrogen abstraction is in fact greater than that for addition to the carbon center over a wide range of temperatures (300−2000 K).

Examining next the preexponential factors for the β-scission reactions, we note that these also lie in a relatively narrow range. In the substituted systems, there is generally a small entropic preference for β-scission of the CH_3−C(X,Y)Z• radicals (i.e., the reverse of addition to the substituted carbon) compared with the β-scission of the •C(X,Y)Z−CH_3 radicals. This is because reaction at the substituted carbon now leads to reduced (rather than increased) steric hindrance. This same effect leads to the slight increase in preexponential factors for this reaction with increasing methyl substitution. For both types of β-scission, the reactions yielding thiocarbonyl compounds have slightly higher preexponential factors than those yielding the carbonyl compounds, which is probably due to greater relief of steric strain in the looser transition structures of the former case. The lowest preexponential factors occur for β-scission to form alkenes, and this is because the alkyl radicals have additional vibrational degrees of freedom to lose upon fragmentation and therefore have a lower vibrational entropy of activation.

In a manner similar to that found for the addition reactions, the relative rates of the β-scission reactions are also dominated by the differences in the barriers. The β-scission reactions of the alkyl radicals have negligible reaction rates at room temperature. Hence, depropagation is not normally a problem in the free-radical polymerization of simple olefinic monomers at normal temperatures (though it can become significant at higher temperatures and in appropriately substituted systems). In contrast, the β-scission of alkyl groups from alkoxy radicals have significant rates at room temperature and indeed are known to be important in atmospheric and combustion chemistry. The β-scission of methyl groups from radicals of the form •C(X,Y)-SCH_3 have low rate constants at room temperature, though they do increase substantially with methyl substitution. Nonetheless, the rate constants of such reactions remain relatively low for some of the typically used RAFT agents, and this can account for the rate retardation that is observed in these RAFT polymerization systems.[4b]

Conclusions

Addition reactions of methyl radical to C=C, C=O, and C=S bonds proceed via early transition structures. The lowest barriers are observed for addition to C=S bonds due to the combination of low singlet−triplet gaps and large exothermicities. The barrier for addition to the carbon center of formaldehyde is lower than for addition to ethylene due to the low singlet−triplet gap, despite having a smaller exothermicity. However, the barriers for addition to carbon in the substituted carbonyl systems are

larger due to increasing singlet−triplet gaps. The barriers for addition of methyl radical to C═C bonds are largely dominated by the reaction exothermicities. Entropic differences among corresponding addition and β-scission reactions are relatively minor, and the differences in reaction rates are thus dominated by differences in the respective reaction barriers.

Addition to the unsubstituted carbon center of C═C double bonds is favored over addition to the substituted carbon center, both thermodynamically (greater exothermicities) and kinetically (lower barriers). This preference for addition to the unsubstituted carbon may be attributed largely to the greater spin density at this site in the triplet state. For the carbonyl systems, addition to the carbon center is also favored thermodynamically and kinetically over addition to the oxygen. Addition to the carbon center of C═S bonds is thermodynamically favored over addition to sulfur. However, addition of methyl radical to the sulfur center proceeds via a lower barrier, and this may be explained in terms of spin density considerations.

Acknowledgment. We gratefully acknowledge generous allocations of computing time on the Compaq Alphaserver of the National Facility of the Australian Partnership for Advanced Computing and the Australian National University Supercomputing Facility and provision of a CONACyT-México postdoctoral fellowship (to R.G.B.), an Australian Research Council (ARC) postdoctoral fellowship (to M.L.C.), and an ARC Discovery grant (to L.R.).

Supporting Information Available: Table S1 contains GAUSSIAN archive entries showing UQCISD/6-31G(d) geometries for all species considered in the present work. Corresponding G3X-RAD//QCISD/6-31G(d) total energies are contained in Table S2. This material is available free of charge via the Internet at http://pubs.acs.org. See any current masthead page for ordering information and Web access instructions.

JA039139A